HOKKAIDO UNIVERSITY

Title	Pilot application of the Volcanic Unrest Index (VUI) for active volcanoes in Japan: Mount Tokachidake and Mount Meakandake
Author(s)	Hashimoto, Takeshi; Aoyama, Hiroshi; Tanaka, Ryo et al.
Citation	Earth, Planets and Space, 78(1), 145 https://doi.org/10.1186/s40623-026-02486-9
Issue Date	2026-06-30
Doc URL	https://hdl.handle.net/2115/100330
Rights(URL)	https://creativecommons.org/licenses/by/4.0/
Type	journal article
File Information	s40623-026-02486-9.pdf

Hokkaido University Collection of Scholarly and Academic Papers : HUSCAP

Earth, Planets and Space

FULL PAPER Open Access

Pilot application of the Volcanic Unrest Index (VUI) for active volcanoes in Japan: Mount Tokachidake and Mount Meakandake

Takeshi Hashimoto[1*], Hiroshi Aoyama[1], Ryo Tanaka[1], Takahiro Ohkura[2], Toshiya Mori[3], Ryo Takahashi[4], Akimichi Takagi[5], Mare Yamamoto[6], Masahiro Ichiki[6], Wataru Kanda[7], Akihiko Terada[7] and Mitsuru Utsugi[8]

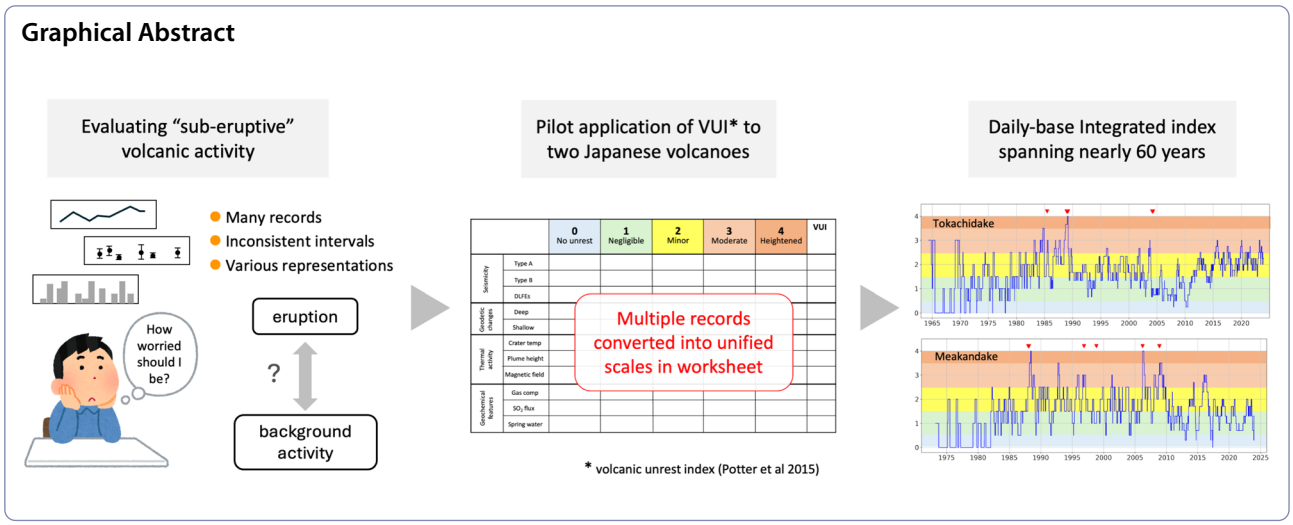
Abstract

The quantitative assessment of volcanic unrest is essential for understanding volcanic processes and supporting decision-making. However, systematic approaches to evaluating unrest episodes remain underdeveloped, particularly during non-eruptive periods. The Volcanic Unrest Index (VUI), originally proposed in New Zealand as a communication tool, condenses diverse monitoring parameters into a single numerical index ranging from 0 to 4, with VUI 4 indicating the highest unrest level. Here we present the first application of the VUI to Japanese volcanoes, focusing on Mount Tokachidake and Mount Meakandake in Hokkaido, and develop an operational framework for its implementation using long-term monitoring datasets. Daily VUI values were constructed from monitoring datasets provided mainly by the Japan Meteorological Agency (JMA). For each data record, scores were assigned using thresholds defined based on proportion-based distributions of assigned scores or, where not applicable, from geophysical or geochemical thresholds. These daily scores were then aggregated into overall VUI values using a hierarchical framework, enabling daily evaluation through a sliding time-window approach across datasets spanning 50 years. The VUI captured episodes of heightened activity associated with eruptions and non-eruptive unrest. At Tokachidake, the VUI exhibited peaks corresponding to the 1985 phreatic eruption, the 1988–1989 magmatic eruption, and the 2004 phreatic event, and reflected prolonged fumarolic activity after 2018. At Meakandake, VUI 4 emerged four times over the study period. Three of these corresponded to the eruptive periods in 1988, 2006, and 2008. Meanwhile, two other eruptions in 1996 and 1998 were not associated with VUI 4, but were instead categorized as VUI 3 and 2, respectively. Integration of multiple parameters reduced responsiveness relative to individual datasets. These results highlight the effectiveness of the proposed framework in providing a consistent, quantitative basis for comparing volcanic activity over multi-decadal timescales, while also underscoring limitations stemming from data availability and averaging across Categories. The study demonstrates that the VUI can serve not only as a framework for systematic evaluation of volcanic unrest in Japan but also as a computational platform for organizing and analyzing sub-eruptive activity, supporting future probabilistic eruption forecasting. Future directions include optimization of evaluation criteria across different volcanic settings and real-time automation.

Keywords Volcanic Unrest Index (VUI), Tokachidake, Meakandake, Volcanic activity evaluation, Multiple data

*Correspondence:
Takeshi Hashimoto
hasimoto@sci.hokudai.ac.jp
Full list of author information is available at the end of the article

© The Author(s) 2026. **Open Access** This article is licensed under a Creative Commons Attribution 4.0 International License, which permits use, sharing, adaptation, distribution and reproduction in any medium or format, as long as you give appropriate credit to the original author(s) and the source, provide a link to the Creative Commons licence, and indicate if changes were made. The images or other third party material in this article are included in the article's Creative Commons licence, unless indicated otherwise in a credit line to the material. If material is not included in the article's Creative Commons licence and your intended use is not permitted by statutory regulation or exceeds the permitted use, you will need to obtain permission directly from the copyright holder. To view a copy of this licence, visit http://creativecommons.org/licenses/by/4.0/.



1 Introduction

The assessment and characterization of volcanic activity provide crucial information that can facilitate decision-making and encourage behavioral change among diverse stakeholders, including residents, government authorities, tourists, climbers, and researchers, by presenting the activity status in a clear and accessible manner (e.g., Johnston et al. 1999). Such assessments are necessary not only during eruptive periods but also during non-eruptive phases, particularly during episodes of unrest. In fact, over any given interval, many volcanoes remain in non-eruptive phases, and the duration of quiescence, including sub-eruptive unrest, often exceeds that of eruptions. Episodes of unrest that become frequent or prolonged can generate social anxiety and affect local economies (e.g., Peers et al. 2021). However, the distinction between background activity and unrest is not always clear, and systematic classification has not yet been sufficiently established. Furthermore, as Moran et al. (2011) pointed out, episodes of activity that are not followed by an eruption tend to be underreported, potentially leading to a biased scientific understanding of volcanic processes.

What constitutes unrest varies from volcano to volcano. Although observational data are diverse, simply listing individual parameters, for example, the number of volcanic earthquakes or sulfur dioxide emissions, does not readily provide information that is meaningful for decision-making, particularly for non-specialists. Despite the accumulation of multi-parameter monitoring data, a systematic framework for integrating these observations and quantitatively evaluating volcanic unrest over extended time periods remains underdeveloped.

To address this gap, this study applies the Volcanic Unrest Index (VUI, Potter et al. 2015a; 2015b) to Japanese volcanoes and develops a time-series framework for the continuous and quantitative characterization of volcanic unrest over multi-decadal timescales. The VUI is a simple and transparent index that summarizes multiple observational parameters into a single numerical value, providing a practical means of describing the state of volcanic activity. This study implements the VUI by introducing a sliding time-window approach to construct continuous time series based on long-term monitoring data.

As part of a research project conducted from 2019 to 2023, we applied the VUI to five well-monitored volcanoes in Japan. In this paper, we focus on Mount Tokachidake and Mount Meakandake in Hokkaido, for which VUI worksheets were developed under a common framework. These volcanoes were selected because they possess long-term observational records, have experienced multiple episodes of eruptions and unrest during the observational period, and are associated with significant levels of human exposure, including tourism and mountaineering. The full calculation workflow is provided in the supplementary spreadsheets (Additional files 1 and 2).

The proposed framework enables systematic and continuous evaluation of volcanic unrest over extended periods, facilitating and providing a basis for future statistical analyses of eruption precursors. At the same time, the approach requires sufficiently long and stable monitoring datasets, ideally encompassing multiple episodes of unrest and quiescence, to establish meaningful statistical thresholds. Accordingly, the present analysis is best suited to well-monitored volcanoes.

In the following sections, we first describe briefly the background of the VUI in relation to the existing system of volcanic alert levels in Japan. Next, we describe the methodology for constructing the VUI worksheets and the criteria used for evaluation. We then examine the

correspondence between the resulting VUI time series and observed volcanic activity, and discuss the strengths and the limitations of the approach, as well as directions for future improvement. The VUI worksheets presented in this study were developed as part of an exploratory analysis. They are not intended for direct use in the current alert system, nor in municipal volcanic disaster management plans.

2 Background

The VUI was developed as a practical framework for characterizing the intensity of volcanic unrest using multiple observational parameters in a structured and transparent manner (Potter et al. 2015a; 2015b). The VUI evaluates the state of volcanic activity over a defined time period by assigning scores to several categories of observations, such as seismicity, deformation, and gas emissions. Each parameter is assessed on a discrete scale, and the overall index is obtained by averaging these values and rounding to an integer, typically ranging from 0 to 4.

One of the key advantages of the VUI is its ability to integrate heterogeneous observational data into a single quantitative measure, facilitating comparison across time periods and between volcanoes. In addition, its relatively simple formulation enhances transparency and interpretability, making it suitable not only for scientific analysis but also for communication with non-specialists. The framework can accommodate datasets with different temporal resolutions and can be adapted for semi-automated or fully automated processing.

At the same time, several limitations of the VUI should be noted. Because the index aggregates multiple parameters, it may reduce sensitivity to short-term or parameter-specific changes. Furthermore, the simplification inherent in reducing complex volcanic processes to a single numerical value can obscure important details contained in individual observations. The selection of parameters and the definition of evaluation criteria therefore require careful consideration, particularly when adapting the framework to different volcanic settings.

The VUI worksheet is not a fixed template and must be tailored to the characteristics of each volcano and the availability of observational data. Previous applications have demonstrated its flexibility in both short-term assessments of discrete unrest episodes and longer-term evaluations based on continuous monitoring records.

A seemingly similar framework for describing volcanic activity is the Volcanic Alert Level (VAL) system used in Japan operated by the Japan Meteorological Agency (JMA). The current VAL is a five-level scheme that, while informed by the state of volcanic activity, is fundamentally oriented toward hazard communication, incorporating expected impacts and recommended actions in coordination with local disaster management authorities (Japan Meteorological Agency 2026). In this sense, the VAL is closely tied to societal response and risk mitigation.

In contrast, the VUI is designed to quantify the state of volcanic activity itself based primarily on observational data, and it is not currently implemented as an official operational tool in Japan. Its framework is constructed independently of hazard or response considerations, focusing instead on the systematic characterization of volcanic unrest.

This distinction is essential for interpreting the role of the VUI in this study: rather than serving as a warning system, it provides a complementary, data-driven framework for describing volcanic activity, which may support but does not replace existing alert systems such as the VAL.

3 Methods

3.1 Basic workflow

The basic structure of the VUI worksheet used in this study follows Potter et al. (2015a; 2015b). Building on this framework, we developed evaluation procedures tailored to Japanese volcanoes. A key modification introduced in this study is the explicit definition of a hierarchical structure, comprising Categories, Items, and Targets, to provide a logical and consistent basis for determining evaluation criteria, which was not fully formalized in the previous studies. The VUI evaluation is hierarchical, progressing from individual data records to Category-level indices and ultimately to the integrated VUI, as illustrated by schematic examples in Fig. 1.

The primary observational dataset relied on long-term, stable records maintained by the JMA. Complementary observations and analyses from other institutions were likewise considered valuable and incorporated into the evaluation whenever feasible. Rather than homogenizing or merging datasets at the raw data level, each dataset was evaluated independently and converted into a standardized index, allowing consistent integration of datasets with different units and measurement characteristics. It should be noted that the different observation types are characterized by markedly different temporal resolutions. Some parameters (e.g., direct gas sampling) being available only at relatively long intervals. We take advantage of the key feature of the VUI, namely its capability of integrate such datasets with differing measurement intervals. When a particular assessment element (Category, Item, or Target) was absent on the evaluation day, it was excluded from the VUI calculation.

We considered four evaluation Categories: seismicity, deformation, thermal activity, and geochemical features for Tokachidake. However, the geochemical Category was

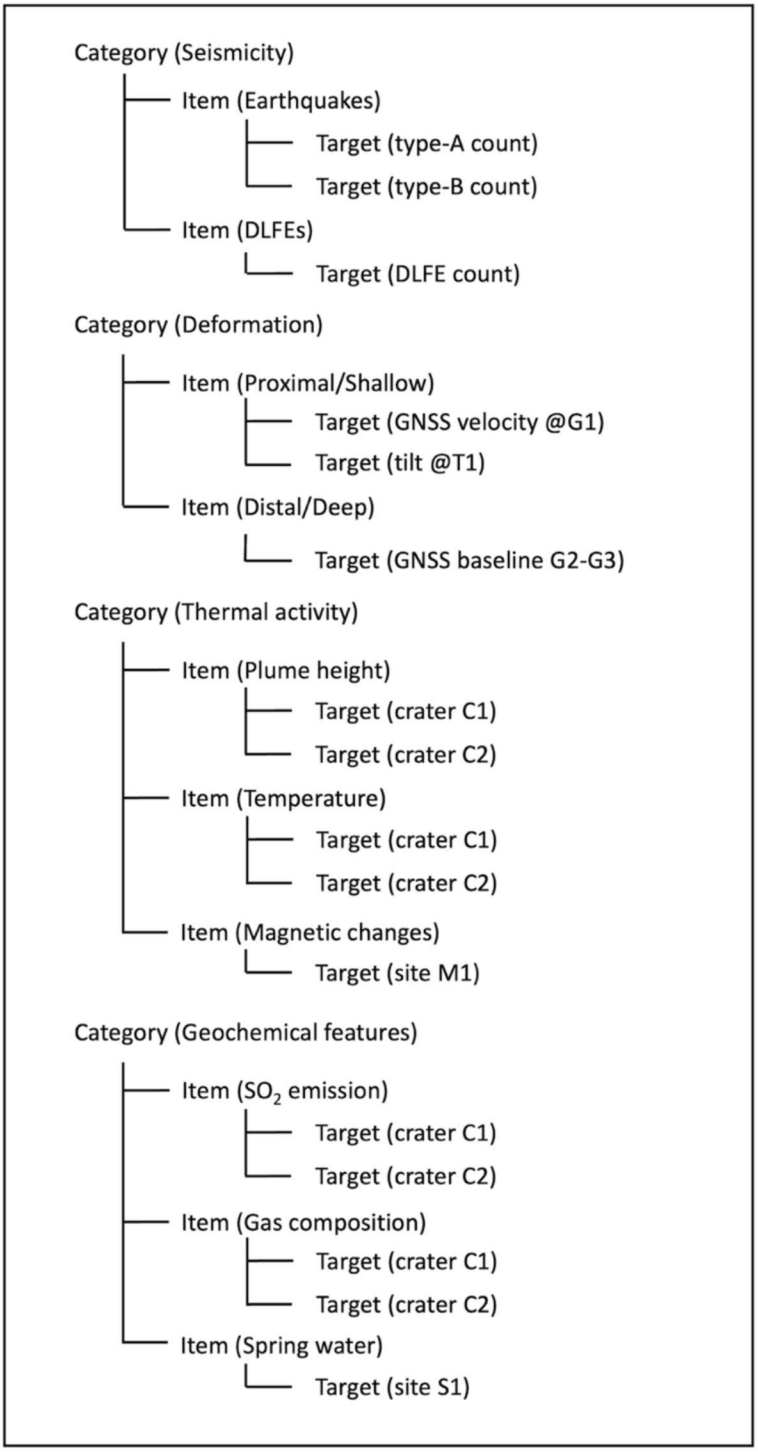


Fig. 1 Conceptual framework of the VUI used in this study. The framework consists of three levels: Categories, Items, and Targets. Each Target represents an individual observational record from which an individual unrest index (iVUI) is derived. The maximum iVUI is selected within each Item, and the maximum Item-level value is selected within each Category to obtain Category-level indices. The overall VUI is then calculated by averaging across Categories. Examples of observational parameters used in this study are shown for each level. This figure does not represent the exact configurations used for Mt Tokachidake or Mt Meakandake

omitted for Meakandake because suitable data records were not available. Each Category comprised one or more assessment Items, when deemed applicable. For example, the "thermal activity" Category for Tokachidake included plume height, crater temperature, and magnetic changes, which collectively reflect the behavior of a dynamic hydrothermal system. For Items with multiple Targets (e.g., multiple craters or observation points), we first assessed each record individually, and then adopted the maximum value to represent the evaluation Item. This choice ensures that localized or migrating activity signals are not overlooked. Integration among Items can, in principle, be performed using either the maximum or the mean; however, in this study, we applied the same maximum-value principle to avoid signal dilution in Categories arising from averaging over a larger number of Items. Finally, the integrated VUI was obtained as the mean across Categories and then rounded to the nearest integer, allowing all Categories, representing different physical and chemical processes to contribute comparably to the final index. Throughout the manuscript, individual unrest indices for each Target, Item or Category are denoted as "iVUI", whereas the plain (unmarked) "VUI" refers either to the integrated index, or more generally to the volcanic unrest index in a broader sense.

We adopted the maximum-value principle within each assessment Item when multiple related records are available. This choice is motivated by the need to capture significant but potentially localized or shifting activity signals, a situation commonly observed in volcanic systems, particularly in thermal, geochemical, and some seismic observations. In such cases, the apparent level of overall activity may remain similar while the locus of activity migrates, and averaging across locations may obscure these signals. For deformation observations and some seismic Items, only a single Target was assigned to each Item and therefore the maximum-value operation had no practical effect. At Tokachidake, the earthquake Item includes both A- and B-type earthquakes, which may reflect different source regions or temporal evolutions of volcanic activity, further supporting the use of the maximum-value principle. By contrast, when integrating the different Categories into a composite VUI, we employed the mean. Since each Category represents a distinct physical process, averaging allows all Categories to contribute to the integrated index in a balanced manner, rather than restricting their influence to an all-or-nothing contribution. It should also be noted that each parameter is first transformed into a standardized iVUI scale (0–4), with thresholds defined so that the frequency distributions are broadly comparable among datasets. This standardization allows different types of observations to be integrated on a common basis. At the intermediate level of integration (Item), either the maximum or the mean could in principle be applied; in this study, however, we adopted the maximum value to ensure that meaningful signals are not overlooked.

In this study, we developed a scheme to calculate daily VUI values, with the prospect of future automation enabling real-time computation on a daily basis. For each record, a 90-day sliding window preceding the target day was defined. This choice follows the original VUI concept (Potter et al. 2015a), which recommends using a sliding time window comparable to the longest interval between regular observations or samples, so that the maximum available parameters are incorporated into the evaluation. In the present dataset, some parameters are observed at intervals comparable to this timescale. In addition, certain unrest phenomena, such as earthquake swarms and ground deformation, may persist over timescales of several months, and once a high iVUI value emerged, a 90-day window allows it sustained for this timescale, even if the relevant activity has temporarily waned. At the same time, it avoids excessive smoothing and retains sensitivity to temporal changes in waning phases. The maximum value within this window was extracted and assigned an iVUI score from 0 to 4 according to predefined criteria. This approach is robust against data gaps: in the absence of larger subsequent values, the same score is retained for approximately 90 days, while waxing activity is promptly reflected.

The choice of a 90-day evaluation window was not based on a strict physical rationale, but rather on practical considerations. Elevated activity is assumed to require monitoring over at least several months, and field observations are typically conducted one to several times per year, mainly between spring and autumn in Hokkaido. Setting the validity period to three months ensures coverage for most of the year. If no data are available within the 90-day evaluation window, the day is treated as missing (#N/A). Extending the window would reduce the number of missing values but was avoided to prevent prolonged reliance on outdated observations.

The evaluation criteria were established primarily according to a proportion-based approach. Thresholds were iteratively adjusted so that the distribution of iVUI values approximates 40% for iVUI 0, 30% for iVUI 1, 20% for iVUI 2, 9% for iVUI 3, and 1% for iVUI 4. This ensures balanced weighting across datasets, while allowing threshold values to differ between volcanoes depending on their characteristics and observational conditions. For some parameters, however, thresholds were defined based on physical or chemical grounds (e.g., boiling point of water for crater temperature, and SO_2/H_2S and SO_2/HCl ratios derived from on-site measurements or direct sampling for volcanic gas composition).

Data requiring extensive modeling (e.g., source parameter calculations) were excluded to maintain simplicity and reproducibility. Since this study prioritized representing the overall magnitude of sub-eruptive volcanic activity based on multiple types of observational datasets, we avoided using specific hazard-related components.

Although the VUI was originally designed as an index for volcanic activity below the eruption level (Potter et al 2015a), we also applied the same criteria to eruptive periods in this study. Here, eruptive activity is treated as the upper bound of the activity spectrum, effectively corresponding to saturation at VUI 4, rather than being used to quantify eruption magnitude. This approach allows for a discussion of the correspondence between eruptive events and the VUI, particularly with regard to their timing. While the VUI is expressed as an integer from 0 to 4 for communication purposes, the non-integer VUI before rounding also has scientific significance as a comprehensive and objective measure of volcanic activity. It retains subtle variations that are lost in the integer VUI through rounding; therefore, we primarily referred to the non-integer VUI when discussing its responses to specific events in later sections. Since the averaging involves three or four Categories, values are meaningful only to the first decimal place.

3.2 Overview of the target volcanoes and data used in the analysis

3.2.1 Mount Tokachidake

The Tokachidake volcanic group is a Quaternary volcanic complex in central Hokkaido. Mount Tokachidake, with an elevation of 2077 m, is one of its edifices and is classified as an active volcano (Figs. 2 and 3). In the twentieth century, it experienced three magmatic eruptions in 1926, 1962, and 1988–1989. The 1926 eruption (VEI 1, based on the Volcanic Explosivity Index; Newhall and Self 1982) caused a partial collapse of the Central Crater Cone, forming the Taisho crater and triggering

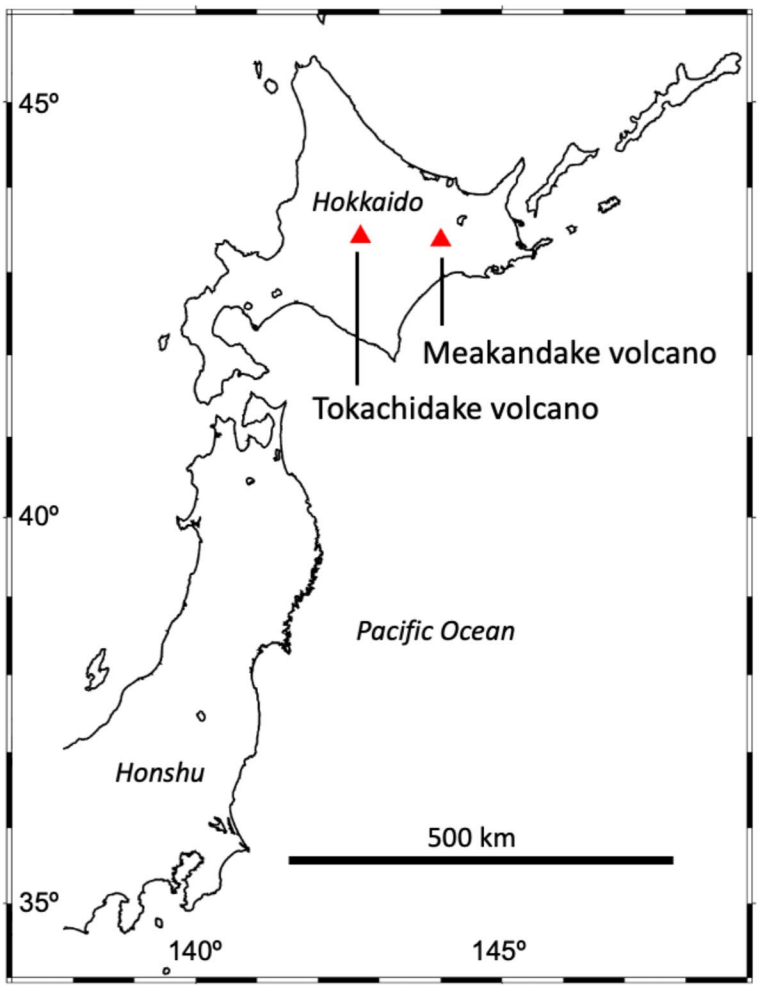


Fig. 2 Locations of Mt Tokachidake and Mt Meakandake (red triangles)

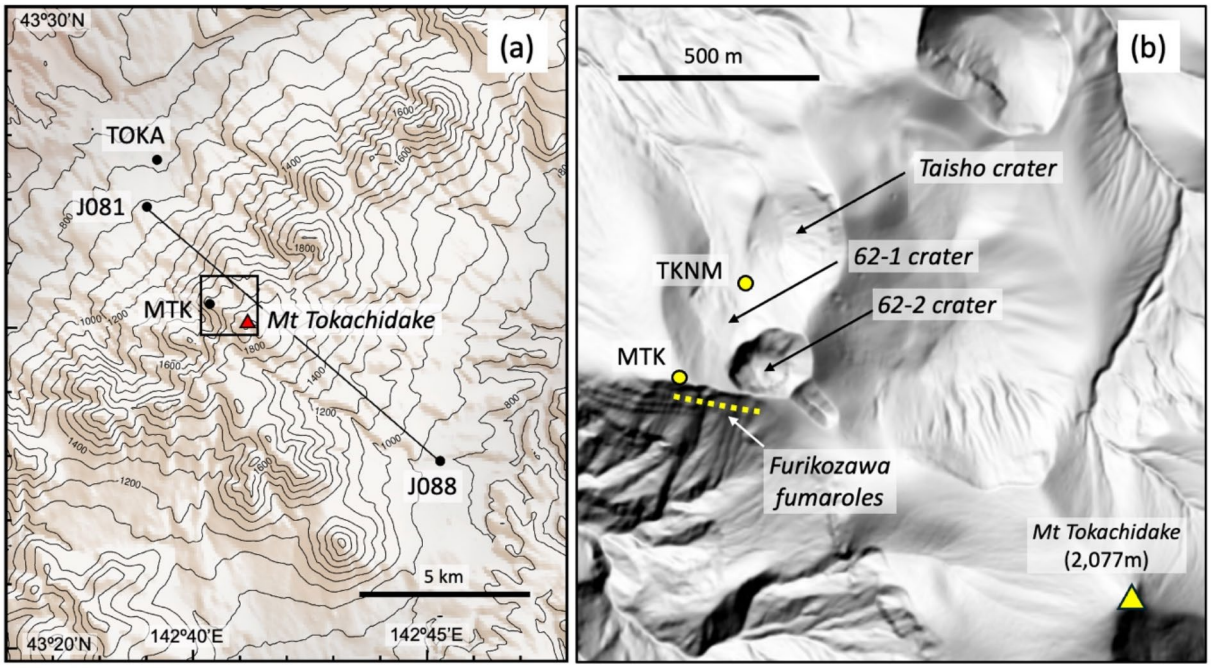


Fig. 3 Topography, major landmarks, and observation sites around Mt Tokachidake. The square in panel **a** shows the area depicted in panel **b**. TOKA: seismic station used for counting earthquakes; J081, J088, and MTK: GNSS stations; The solid line connecting the J081 and J088 stations indicates the baseline used to evaluate the crustal deformation; TKNM: geomagnetic station

large-scale debris flows. The 1962 event was a major eruption (VEI 3) from the southern part of the Central Crater Cone, generating an ash plume that reached 12 km in height and forming multiple craters, including the 62–2 crater, which continues fumarolic activity to the present. The latest magmatic eruption occurred at the 62–2 crater in 1988–1989. A minor phreatic eruption took place at the same crater in 2004, and no eruptions have been observed since then (Japan Meteorological Agency 2013).

Significant ground deformation indicative of shallow inflation near the 62–2 crater was detected between 2006 and 2017. Beginning around 2018, fumarolic activity at both the 62–2 crater and the Furikozawa fumarole field progressively intensified, continuing until about 2021. Seismicity, although fluctuating since roughly 2010, has remained at generally elevated levels (Additional file 3: Figs. S1–3). Since 2018, shallow ground deformation has shifted to contraction; nevertheless, notable fumarolic activity persists at the Taisho crater, the 62–2 crater, and the Furikozawa fumarole field as of 2025.

More than 35 years have passed since the most recent magmatic eruption at this volcano. Although such a duration alone does not necessarily indicate elevated concern, the magmatic eruptive history since the twentieth century suggests that it is approaching the range of past inter-eruption intervals. Continuous monitoring by the JMA has been conducted at Tokachidake since the mid-1960s. The JMA provided the data for seismicity, deformation, plume height, crater temperatures, and part of the SO_2 flux measurements. The following section describes the datasets used in this study to construct the VUI worksheet in detail. The locations of the observation sites are shown in Figs. 2 and 3.

3.2.1.1 Seismicity Among the various monitoring activities conducted at Tokachidake, seismic observation has the longest history. In this study, we analyzed daily earthquake counts since 1970 obtained at the JMA's Iwozawa station (station code: TOKA). The JMA classifies volcanic earthquakes into different types using multiple lines of information, including waveform characteristics, hypocentral location, and S-P time (i.e., the time difference between the arrivals of P and S waves). In JMA operational procedures, volcanic earthquakes are identified using criteria including amplitudes ≥ 0.05 μm and S-P times ≤ 2 s. S-P time is also used as a proxy for source distance or depth when precise hypocenter determination is difficult. In this study, we used the events classified by JMA as type A (high-frequency volcano-tectonic earthquakes) and type B (low-frequency events typically associated with fluid movement) (Minakami 1960). Type A earthquakes generally represent activity at relatively greater depths, whereas type B corresponds to shallower activity

immediately beneath active craters. In this study, seismicity is defined as the total number of volcanic earthquakes reported by the JMA. Although the operational procedure does not strictly define a fixed spatial boundary, these events effectively correspond to seismicity occurring within an area of approximately 20×20 km around the volcano, representing the typical extent of monitored volcanic seismicity. Both types typically occur fewer than 100 times per year on average, and days without any detected events are common. To capture low-level background activity during quiescent periods, we calculated a 15-day cumulative count for each day. The iVUI values for type A and type B were evaluated separately using the maximum value within the preceding 90-day window (Additional file 3: Fig. S1).

More advanced seismic parameters such as Real-time Seismic Amplitude Measurement (RSAM; Endo and Murray 1991) and Displacement Seismic Amplitude Ratio (DSAR; Caudron et al. 2019) were not included, as they require consistent reprocessing of continuous waveform data, which is not uniformly available over the full observation period considered in this study.

3.2.1.2 Deformation This Category incorporates two types of data records. The first consists of daily Global Navigation Satellite System (GNSS) positions of station MTK, located approximately 200 m west of the 62–2 crater. MTK was originally installed and operated by the Hokkaido Research Organization (HRO) and Hokkaido University, and since 2022 has been taken over by the JMA. The daily positions, calculated relative to the Bougakudai station (J081, approximately 3 km northwest of the crater area), are available for the period from 30 May 2003 through the end of 2023. Only the horizontal components were considered in this study.

To suppress noise and outliers, a 15-day moving median was applied. Subsequently, the slope, i.e., the horizontal displacement rate, was estimated daily using a linear fit over a 365-day moving window. The maximum slope within the preceding 90 days was then evaluated and converted into iVUI (Additional file 3: Fig. S2a–d). The use of a one-year window reflects the challenging observational environment at MTK: during winter, snow frequently covers the solar panels, causing prolonged data outages. Data quality often deteriorates around such gaps, sometimes producing spurious slopes; shorter windows were found to exaggerate these effects and artificially elevate iVUI values. To address this issue, we adopted the one-year window despite its lower temporal responsiveness. Nevertheless, characteristic events, such as the enhanced activity in 2009 and 2012 and the abrupt change in 2016, are adequately captured in the displacement-rate record. For volcanoes with more stable datasets and fewer gaps, shorter window lengths may be used without concern.

The second dataset consists of long GNSS baseline measurements spanning the volcano, provided by the JMA. Specifically, the baseline between the JMA stations at Bogakudai (J081) and Yunotaki (J088; ca. 7 km southeast), with a length of approximately 11 km, has been available since August 2011. The same processing procedure as the MTK record was applied to this dataset: a 15-day running median was used, followed by the calculation of the annual slope, and the maximum value over the preceding 90 days was evaluated (Additional file 3: Fig. S2e–g). While the MTK station reflects shallow sources directly beneath the crater, the J081–J088 baseline is considered to capture pressure variations at greater depths.

3.2.1.3 Thermal activity Thermal activity was evaluated in three assessment Items: plume height, crater temperature, and rock demagnetization around the craters.

First, plume height is based on JMA's distant observations since 1964. Plume heights were determined visually or from video footage, and three Targets were considered, corresponding to the 62–2 crater, Taisho crater, and the Furikozawa fumarolic zone. Among these, the 62–2 crater generally dominates, with plume heights exceeding 100 m for most of the observation period. The absence of data for the Furikozawa fumaroles between 2008 and 2015 indicates that plume activity had declined below the detection limit of distant observations. From 2016 onward, numerous fumaroles have been observed in this area, and maximum plume heights exceeding 50 m have become relatively common. Plume height data are often missing due to poor weather conditions, and daily values exhibit substantial variability due to wind. Therefore, the plume height data provided by the JMA were available as monthly values, defined as the average of daily maxima for each month. In this study, the data were assigned to the last day of each month, and the iVUI was evaluated for each plume using the maximum value over the preceding 90 days (Additional file 3: Fig. S3).

Second, for crater temperature records, we utilized measurements collected during on-site surveys conducted by the JMA and HRO since 1971. Observations were generally performed twice a year, in spring and autumn. In this study, thermal infrared observations at the 62–2 crater and the direct measurements at the 62–1 and Taisho craters, provided by the JMA and HRO, were used to evaluate the iVUI based on the maximum temperature over the preceding 90 days (Additional file 3: Fig. S4).

Third, we incorporated total geomagnetic field intensity data recorded at station TKNM, which was set up

by Hokkaido University in 2014 (see Fig. 3 for the location). This site is located approximately 300 m northwest of the 62–2 crater and designed to monitor thermal de/re-magnetization beneath the crater. Measurements were performed automatically at 15-min intervals. Previous studies based on the repeated magnetic surveys (e.g., Hashimoto et al. 2010), reported thermal demagnetization at a shallow level beneath the 62–2 crater. In the present study, assuming that the source location remains largely unchanged, we interpreted increases in total magnetic field intensity at TKNM as an indicator of thermal demagnetization beneath the crater. Here, variations in total intensity were evaluated as reflecting either a rise in temperature or heat accumulation beneath the crater. To remove geomagnetic field variations of extra-terrestrial origin, the data were corrected by subtracting simultaneous total intensity values at a reference site (MTY, located approximately 200 km southwest of Tokachidake). Outliers were then removed by excluding data deviating by more than ± 20 nT from the median value of the analyzed time-series segment, and daily means were calculated. We computed the rate of change over 100 days and evaluated the iVUI using the maximum value over the preceding 90 days. In addition to long-term demagnetization trends throughout the observation period, shorter-term variations on the order of several months to one year were also observed (Additional file 3: Fig. S5).

3.2.1.4 Geochemical features Our evaluation of geochemical characteristics was based on three assessment Items: volcanic gas composition, SO_2 flux in volcanic plumes, and the contribution of deep hydrothermal fluid to hot spring waters.

First, volcanic gas composition was determined from open-file reports published by the Geological Survey of Japan (Shinohara et al. 2025), which provide chemical analysis data of gas samples collected directly in the field. Because these data are highly sporadic in time, proportion-based criteria were not applied. Instead, the degree of magmatic contribution was assessed using semi-quantitative criteria, derived from molar ratios of individual gas components. These criteria were developed with reference to the classification of fumarolic gas compositions proposed by Ozawa (1965). While his classification only qualitatively shows the relative abundances of the components, we introduced specific threshold values for the component ratios for practical purposes in calculating the iVUI as shown in Table 1. For consistency with other parameters, the iVUI was defined as the maximum value within the 90 days preceding each evaluation date. In practice, this means that each gas analysis remains valid for 90 days after the sampling date. At Tokachidake, the available gas composition data always yield iVUI values ranging from 2 to 4, indicating that a magmatic signature has been maintained throughout the analyzed period (Additional file 3: Fig. S6a).

Table 1 Criteria for chemical component ratios in volcanic gases

iVUI	Criteria (molar ratio)	Note
4	$5 < (SO_2/H_2S)$	Type I of Ozawa (1965)
3	$2 < (SO_2/H_2S) <= 5$	
2	$0.2 < (SO_2/H_2S) <= 2$ and $(SO_2/HCl) <= 5$	Type II of Ozawa (1965)
1	$0.2 < (SO_2/H_2S) <= 2$ and $5 < (SO_2/HCl)$	Type III of Ozawa (1965)
0	$(SO_2/H_2S) <= 0.2$	Type IV of Ozawa (1965)

Next, the SO_2 flux data were all derived from ultraviolet spectroscopic measurements. The dataset includes previously published results (Mori et al. 2006; Carn et al. 2017; Yamaguchi et al. 2023), observational data provided by the JMA, and additional data collected and analyzed by Hokkaido University and the University of Tokyo. Ground-based measurements were conducted using both traverse and scanning techniques. The dataset reported by Carn et al. (2017) is based on remote sensing with the Ozone Monitoring Instrument (OMI) satellite sensor, and the original values are given as annual emission rates. For the purposes of this study, these values were converted into daily fluxes and assigned to June 30 of each year. Since 2019, most of the available data have come from remote sensing estimates using the Tropospheric Monitoring Instrument (TROPOMI) satellite sensor, as reported by Yamaguchi et al. (2023). Further details about the datasets are provided in the accompanying worksheet (Additional file 1). With the exception of the Carn et al. (2017) dataset, the SO_2 flux data consist of daily measurements. These daily values are highly variable, largely due to meteorological conditions. To reduce this variability, we applied a 50-day running median to the raw data, and then used the maximum value within a 90-day window to evaluate the iVUI (Additional file 3: Fig. S6b, c).

The evaluation criteria for this Item were established not from proportion-based approach but from physical and volcanological considerations. Sustained SO_2 fluxes above 100 tons per day (t/d) are widely interpreted as clear evidence of magmatic degassing (Symonds et al. 2001). Meanwhile, fluxes exceeding 1000 t/d place a volcano within the top 15% of the 91 passive degassing giants compiled by Carn et al. (2017), a level regarded as indicative of an intensive magmatic contribution. Although 100 t/d was considered an important volcanological reference level, it was not used directly as an iVUI threshold. Instead, intermediate thresholds of 200 t/d and 500 t/d were adopted, dividing the range between 100 and 1000 t/d into three roughly equal intervals on a logarithmic scale, corresponding to iVUI levels 1/2 and

2/3, respectively. In addition, 5 t/d was chosen as the iVUI 0/1 threshold, reflecting the approximate detection limit of ground-based spectroscopic techniques (e.g., walking traverse observations conducted near the crater). At Tokachidake, which ranks 73rd among the 91 passive degassing volcanoes listed by Carn et al. (2017), annual mean fluxes during sub-eruptive periods average 135 ± 98 t/d. Values above 100 t/d are therefore relatively common.

Finally, we address the supply rate of deep hydrothermal fluids to hot spring waters. The HRO samples hot spring water from the middle flanks of Tokachidake approximately every three months for monitoring purposes. A marked increase in Cl concentrations in hot spring waters was observed prior to the 1988–89 eruption (Takahashi et al. 2015). In this study, we estimated the supply rate of ca. 280 °C NaCl-type deep hydrothermal fluid based on the two-component mixing model for the hydrothermal system proposed by Takahashi et al. (2015; 2019). Takahashi et al. (2019) reported estimates up to 2018, and we extended the dataset by applying the same model to subsequent HRO's measurements. As shown in the time-series plot (Additional file 3: Fig. S6d), the supply rate rose to a maximum of 92 L/min before and during the 1988–89 eruption, but then rapidly decreased within about two years. Since August 1992, the rate has remained below ca. 5 L/min up to 2023, except for temporary increases in 2001, 2009, and 2010–2013.

Because the iVUI evaluation of this Item is based on the maximum value within the preceding 90 days, and water sampling is conducted only once every three months, each observation virtually remains valid for the following 90 days. This introduces a degree of temporal persistence in the index, such that short-term increases in activity may not be immediately reflected unless new sampling is made, and the evaluation may be influenced by earlier measurements. Consequently, rapid changes in unrest may be smoothed in the iVUI time series, and the results should be interpreted with this limitation in mind.

It should also be noted that these estimates are based on the above-mentioned two-component mixing model for simplicity and do not rely on direct measurements of the deep hydrothermal fluid itself. The resulting supply rate values are therefore discrete due to a resolution limit and tend to cluster with identical values at low levels. Consequently, proportion-based thresholds are not appropriate, and specific thresholds were defined for this dataset (e.g., iVUI 4 for supply rates exceeding 90 L/min; see Additional file 1).

3.2.2 Mount Meakandake

Mount Meakandake (elevation 1499 m) is a post-caldera stratovolcano located in the southwestern part of the Akan Caldera in eastern Hokkaido (Figs. 2 and 4). The volcanic complex comprises multiple edifices including Ponmachineshiri, Nakamachineshiri, and Akanfuji. The most recent magmatic eruption occurred approximately 1 ka, while all historical eruptions (with the earliest recorded in 1955) have been small-scale (VEI 0–1) phreatic events. The 1998 eruption is the only case in which a magmatic contribution has been suspected (Japan Meteorological Agency 2013).

During the study period from 1973 to 2023, eruptions occurred at the Ponmachineshiri crater in 1988, 1996, 1998, 2006, and 2008. In contrast, no eruptions have been documented at the Nakamachineshiri crater during the same period (Japan Meteorological Agency 2013). A notable feature of recent activity is the occurrence of earthquake swarms exceeding 100 events per day, which have repeatedly taken place several months prior to phreatic eruptions.

At depths of 15–30 km beneath Meakandake, a seismically active zone of deep low-frequency earthquakes (DLFEs) is present, with occurrence rates considerably higher than those at Tokachidake. Previous studies (Kurihara and Obara 2021; Takahashi et al. 2012) have suggested that swarms of DLFEs may be associated with subsequent shallow earthquake swarms and eruptions. Based on these findings, DLFEs were included in the seismic activity Category in this study.

Geochemical analyses have been performed only sporadically over time, and no data suitable for day-to-day VUI evaluation were available; accordingly, a geochemical Category was not defined for this volcano. Although satellite-based observations can provide useful constraints on volcanic gas emissions such as SO_2 when emission rates are sufficiently high, their sensitivity to low-level or intermittent degassing is limited, and detailed geochemical compositions are difficult to retrieve on a daily basis. The future incorporation of chemical indicators would be desirable. For the ground deformation (changes in GNSS baseline length), we digitized the graphs published by the JMA (Sapporo Regional Headquarters, Regional Volcano Monitoring and Warning Center 2024). For the other observational parameters, we used numerical data provided directly by the JMA. The locations of the landmarks and observation sites are shown in Fig. 4.

3.2.2.1 Seismicity In the seismicity dataset of the JMA, A-type earthquakes are the most common, followed by BH-type (high-frequency B-type) events. Because earthquake type identification for Meakandake is relatively difficult and can depend on the judgment of individual analysts, this study did not distinguish between earthquake types. Instead, we used the total daily count of all reported events, as determined by the JMA's volcano monitoring

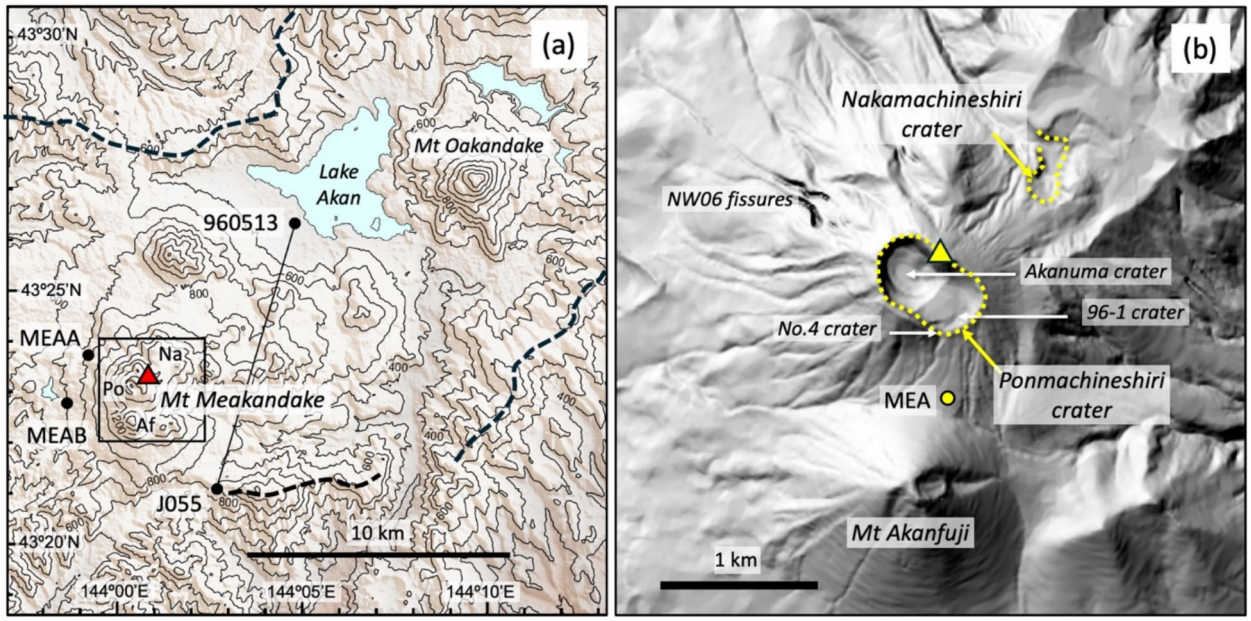


Fig. 4 Topography, major landmarks, and observation sites around Mt Meakandake. The square in panel **a** shows the area depicted in panel **b**. Black broken lines in panel **a** indicate the rim of the Akan caldera (Hasegawa et al. 2009). Po, Na, and Af denote the edifices of Ponmachineshiri, Nakamachineshiri, and Akanfuji, respectively. Yellow broken lines in panel **b** delineate crater boundaries. MEAA and MEAB: seismic stations used for counting earthquakes; J055 and 960,513: GNSS stations; The solid line connecting the J055 and 960,513 stations indicates the baseline used to evaluate the crustal deformation; MEA: geomagnetic station

network (Additional file 3: Fig. S7a). In practice, these events correspond to seismicity occurring within an area of approximately 15×15 km around the volcano, which represents the typical spatial extent of monitored volcanic activity in this region. Following some preliminary testing, the evaluation metric was defined as the sum of the five highest daily counts within the preceding 90 days (Additional file 3: Fig. S7b). For reference, we also evaluated the data using the same 15-day cumulative counts that were applied to Tokachidake. The results, presented as Method 1 in Additional file 2, show an overall trend similar to that of Method 2 (top-5-based) used in this study, though with some differences in the occurrence of levels 3 and 4. It should be noted that the JMA's counting criteria for this volcano have undergone several revisions, and major system changes implemented around 2001, including the switch of the primary counting station from MEAA to MEAB, may have introduced discontinuities in detection capability.

For DLFEs, we used daily counts detected and classified by the JMA. By the end of 2023, a total of 1670 DLFE events had been recorded. Events prior to July 1994 were identified from analog seismogram records, whereas those after August 1994 were based on digital recordings. Because event counts before 2003 are substantially lower than in later years, the consistency of detection capability during the earlier period remains uncertain. In the current study, DLFEs were evaluated using the maximum 15-day cumulative count within a 90-day window, consistent with the procedure applied to ordinary volcanic earthquakes (Additional file 3: Fig. S7d). However, owing to their much lower occurrence rates, more than 56% of days still registered zero events under this metric. As a result, the proportion of each iVUI value (0–4) deviates from the standard configuration (see the worksheet in Additional file 2 for details).

3.2.2.2 Deformation Ground deformation was assessed using GNSS baseline length data. The analyzed baseline is ca. 10 km long, spanning from GEONET station 960513 operated by the Geospatial Information Authority of Japan (GSI), located approximately 8 km northeast of Meakandake, to the JMA station J055, approximately 5 km to the southeast (Fig. 4a). Displacement values were referenced to April 1, 2010, which was set to zero.

To reduce noise and estimate deformation rates, slopes were derived using linear regression within a 60-day moving window, and the maximum slope over the preceding 90 days was adopted as the evaluation metric. This analysis revealed pronounced baseline extension from roughly 2015 to 2019, followed by smaller oscillations superimposed on a long-term contractional trend (Additional file 3: Fig. S8). Although this activity did not culminate in an eruption, it

produced significant deformation on Meakandake's northeastern flank. An Interferometric Synthetic Aperture Radar (InSAR) analysis by Geospatial Information Authority of Japan (2018) indicates that the deformation between October 2016 and May 2017 can be explained by the opening of a sill-like crack, oriented northeast–southwest at a depth of ca. 6 km between Meakandake and Oakandake.

Given these findings, GNSS baseline length was incorporated as an evaluation parameter in the present study, as it reflects volcanic processes associated with pressure changes at depth. The evaluation criteria were defined such that higher rates of baseline change correspond to higher iVUI values. Note that no correction was applied for regional stress fields associated with plate motion.

3.2.2.3 Thermal activity Three types of thermal activity Items were considered: plume height, crater temperature, and geomagnetic variations.

Plume height observations were drawn from four vent systems: the Ponmachineshiri crater (the 96–1 crater), the Akanuma crater, the Nakamachineshiri crater, and the fumarolic fissures to the northwest of Ponmachineshiri that formed during the 2006 eruption (NW06). Daily plume height records form the basis of this dataset. Although intermittent remote visual observations date back to the 1950s, the present study relies on the systematic measurements initiated by the Kushiro Local Meteorological Observatory in 1982. Until 2003, observatory staff conducted binocular surveys twice a day, at 09:00 and 15:00 Japan Standard Time (JST), to record plume heights. Since the installation of a video camera system in 2003, however, the dataset has instead consisted of the highest plume height observed within each 24-h period.

For each crater, the daily maximum plume height was smoothed with a 7-day moving average. Seasonal effects were then corrected by applying a linear regression based on correlations with atmospheric temperature at the Kushiro Local Meteorological Observatory, about 50 km southeast of Meakandake. Atmospheric humidity may also influence plume height; however, this effect was not explicitly considered in the present analysis. The correction coefficient was derived from the 2010–2023 record, a period of relatively low volcanic activity. The evaluation metric was then applied to the maximum value within the previous 90-day time window. It should be noted that seasonal variation was minimal and the correlation with air temperature was weak, so the correction had little practical impact as for the NW06 fumarolic fissures. To prevent any single crater from dominating the results, crater-specific thresholds were adjusted so that the proportion of each iVUI value followed the standard configuration. The iVUI for this Item was taken as the maximum across all four crater iVUIs (Additional file 3: Fig. S9).

For crater temperatures, records from the 96–1 and No. 4 craters (both within the Ponmachineshiri crater) collected by the JMA were used. Regarding the Nakamachineshiri crater, observational data exist only for certain past periods; no continuous field measurements have been conducted since then. At the No.4 crater, direct thermometer measurements have been conducted since May 1997, while earlier observations relied on infrared radiation thermometers. Time series plots of individual crater temperatures, together with their corresponding iVUIs, are presented in Additional file 3: Fig. S10.

Subsurface demagnetization was evaluated using changes in the total magnetic field from a JMA's continuous monitoring station (site name: MEA), located approximately 500 m south of the 96–1 crater (Fig. 4b). Geomagnetic fluctuations of extraterrestrial origins were reduced through preprocessing by the JMA using reference data from the Memambetsu Geomagnetic Observatory (site name: MMB). Takahashi et al. (2018) further incorporated repeat magnetic survey data collected between 2004 and 2014, dividing volcanic activity into several phases and inferring thermal de/re-magnetization sources. The sources were located at depths of several hundred meters, approximately halfway between the 96–1 crater and the MEA station. Within this framework, observed decreases in total magnetic field at MEA are interpreted as corresponding to heating (demagnetization) at the source region. We quantified demagnetization rates as slopes (with inverted sign) calculated over a 60-day moving window. The maximum slope within the preceding 90-day time window was adopted as the evaluation metric (Additional file 3: Fig. S11), where slope values smaller than 0.2 nT/yr were evaluated as iVUI 0. Although Takahashi et al. (2018) reported that the source location may have shifted slightly over time, a single consistent criterion was applied across the entire record to avoid complicating the evaluation scheme.

4 Results

4.1 Mount Tokachidake

At Tokachidake, observational data were initially limited to crater temperatures. By the mid-1980s, additional observational parameters had been introduced, bringing the number of Items (the intermediate level of the assessment hierarchy) to three or four. From the 2000s onward, monitoring expanded further, enabling evaluations based on as many as nine Items, with up to four Categories (the top level of the assessment hierarchy) contributing to the averaging process (Fig. 5a). This broadening of the observational basis, as reflected in the non-integer (i.e. pre-rounded) VUI plot (Fig. 5f), produced a marked

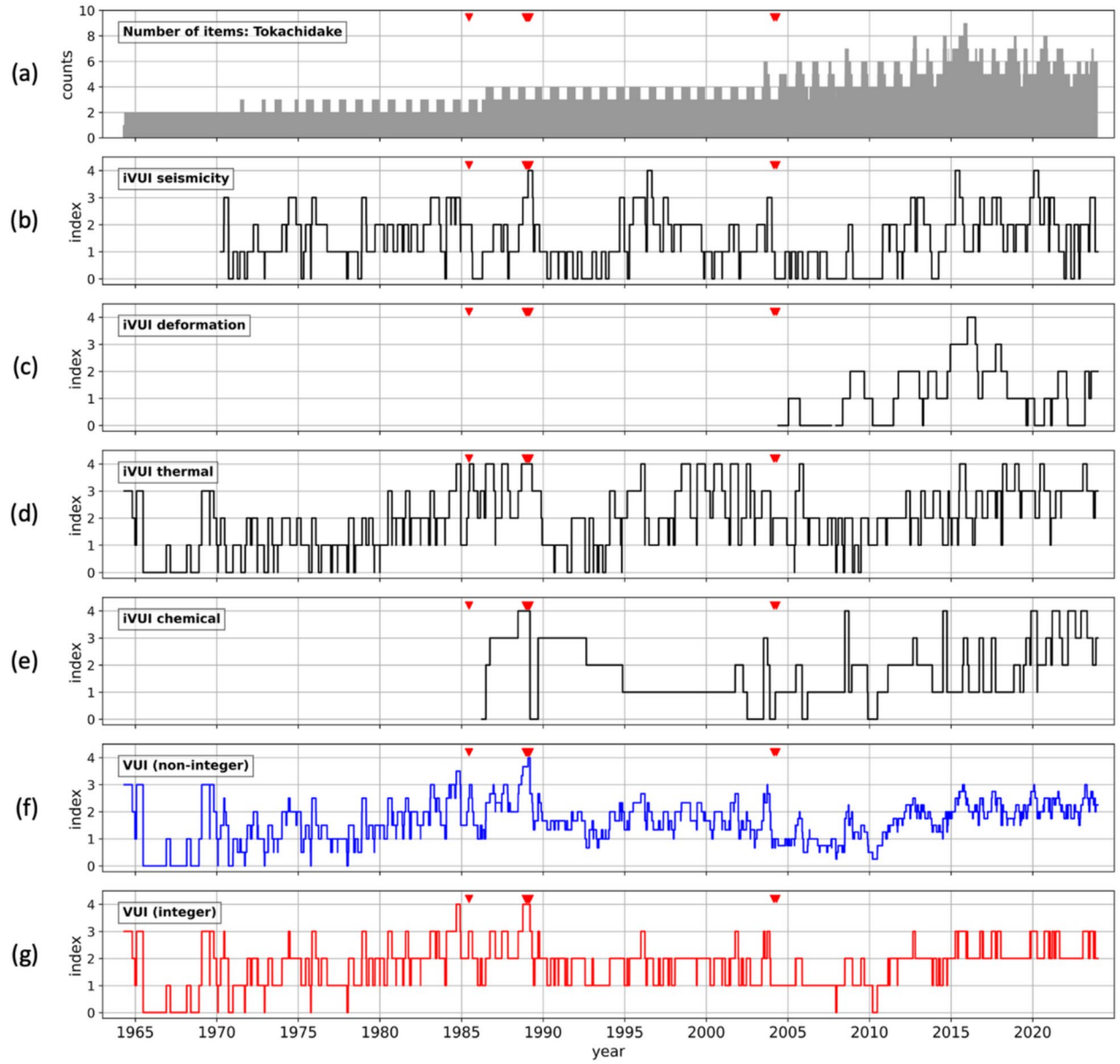


Fig. 5 Time series plots of analyzed results for Mt Tokachidake. **a** Number of assessment Items; **b** Seismicity index; **c** Ground deformation index; **d** Thermal feature index; **e** Geochemical feature index; **f** Integrated VUI (non-integer); **g** Integrated VUI (rounded to integer). Inverted red triangles indicate the timing of eruptions

smoothing of temporal variations from the mid-1980s onward.

An overview of the entire study period, based on the non-integer VUI plot (Fig. 5f), reveals several salient features. From the 1970s through the late 1980s, values rose gradually, culminating in a peak of 4.0 during the later stage of the 1988–1989 eruptive episode. As the eruption waned in March 1989, the index quickly declined, reaching a minimum in 1993. It fluctuated between 1 and 2 between 1993 and 2003, except for a brief rise to 3.0 in autumn 2003, followed by a rapid drop back to 0.7 by early 2004. Even during the minor eruptive phase of February–April 2004, the index did not exceed 1, and low levels generally persisted until around 2007 with a minimum of 0.3. Beginning in mid-2008, however, the VUI began to rise again, showing an upward trend until about 2016. Thereafter, values remained broadly within the range of 1.5 to 3.0 through the end of 2023.

Examining temporal variations of the VUI in relation to past eruptions is essential for understanding what

the index represents and how it evolves. Here, we compare the VUI time series with individual eruptive events shown in Fig. 5. At Tokachidake, a small phreatic eruption occurred in May–June 1985, generating hot muddy water, a pit crater approximately 10 m in diameter, and minor ash fall. The VUI had been on an upward trend since the 1970s, reaching 3.5 (rounded to 4) in November 1984, but it declined to 2.0–2.5 at the time of the eruption (Fig. 5f). This sharp drop occurred because high crater-temperature data (475 °C) at September 1984 field observation fell outside the evaluation window (Fig. 5d and Additional file 1). If successive close-interval temperature data had been available, the integer VUI might have stayed at level 4 during the eruption.

During the 1988–89 eruption period, a good correspondence was observed between the VUI and volcanic activity. In the first half of 1988, the VUI remained at 2.0, but it began to rise in June. By early September, field observations recorded a crater temperature rated as iVUI 4 (Additional file 3: Fig. S4), which contributed to an increase in the overall VUI to 3.3. In early October, roughly two months prior to the eruption, the rise in A-type seismicity (from iVUI 2 to 3; Additional file 3: Fig. S1a-b) coincided with the pre-rounded VUI reaching 3.7, at which point the integer VUI increased from 3 to 4 (Fig. 5g). Although crater-temperature data fell outside the evaluation window by the end of the year, the VUI remained elevated due to an increase in plume height to iVUI 4 (Additional file 3: Fig. S3d), followed by seismic activity also reaching iVUI 4 in January 1989 (Additional file 3: Fig. S1b), resulting in a maximum non-integer VUI of 4.0 at the end of that month. Subsequently, the VUI declined rapidly with the cessation of eruptive activity, falling to 1.3 by June 1989.

A small phreatic eruption occurred on 25–26 February 2004, followed by the observation of plumes containing volcanic ash and low-amplitude volcanic tremor from the 62–2 crater on 19 April. Prior to this eruption, the non-integer VUI had risen from 2.3 to 3.0 in September 2003 in response to heightened seismic activity. However, by late November, sporadic chemical observations, including SO_2 flux and gas composition data, fell outside the evaluation window (Additional file 3: Fig. S6), causing the non-integer VUI to decrease to 2.0. Subsequent quiescence in seismic activity further contributed to a decline, and it had dropped to 1.0 by the time of the eruption. This case illustrates that, when part of the evaluation depends on sporadically available observations, the exclusion of such data from the evaluation window can substantially affect the integrated VUI.

Looking at the entire evaluation period in Fig. 5, peaks in the non-integer VUI are observed around the three eruptive periods of 1985, 1988–89, and 2004. Among these, the peak during the 1988–89 eruption is the highest, and the recent state since 2015 is comparable to the peak observed in 2004.

4.2 Mount Meakandake

The monitoring record at Meakandake initially consisted only of seismicity. By the 1980s, plume height and crater temperature had been added, bringing the number of assessment Items to three or four by the mid-1980s. The dataset expanded further in the 2000s, when GNSS and geomagnetic observations were incorporated, allowing assessment with up to six Items, with a maximum of three Categories contributing to the averaging (Fig. 6 and Additional file 2).

The non-integer VUI plot (Fig. 6e) showed a distinctly stepwise and scattered pattern in the 1970s, reflecting its reliance on seismicity alone. In contrast, the integration of multiple Categories from the 2000s onward produced smoother fluctuations. Long-term changes in the VUI over the studied period broadly reflected the trends of seismicity (Fig. 6b and Additional file 3: Fig. S7) and plume height (Fig. 6d and Additional file 3: Fig. S9e). This is perhaps unsurprising, as data seismicity and plume height have been monitored for longer periods than other parameters and therefore provide more consistent long-term records.

Of the 18,538 days for which the integrated index was calculated, VUI 2 (minor unrest) accounted for 42% of the total. Considering that Meakandake is characterized by persistent fumarolic activity and background seismicity exhibiting temporal fluctuations, this prevalence appears reasonable. As shown in Fig. 6f, VUI 4 (heightened unrest) was recorded on four occasions over the past 50 years (1988, 1992, 2006, and 2008–2009), encompassing a total of 391 days (2.1% of the entire dataset). In three of these instances, excluding 1992, elevated VUI values corresponded to periods of increased activity associated with eruptions. However, the correspondence between eruptions and the highest VUI values is not always straightforward. This reflects the fact that the VUI is designed to represent the overall level of volcanic unrest rather than to directly indicate the occurrence or magnitude of eruptions. Consequently, a one-to-one correspondence is not necessarily expected: sudden or short-lived eruptions may occur without strong or sustained precursory signals, whereas elevated VUI values may arise from prolonged unrest involving multiple parameters without culminating in an eruption. This characteristic should be considered when interpreting and communicating the VUI time series results. In the following, the correspondence between individual episodes and the VUI time series is examined in detail.

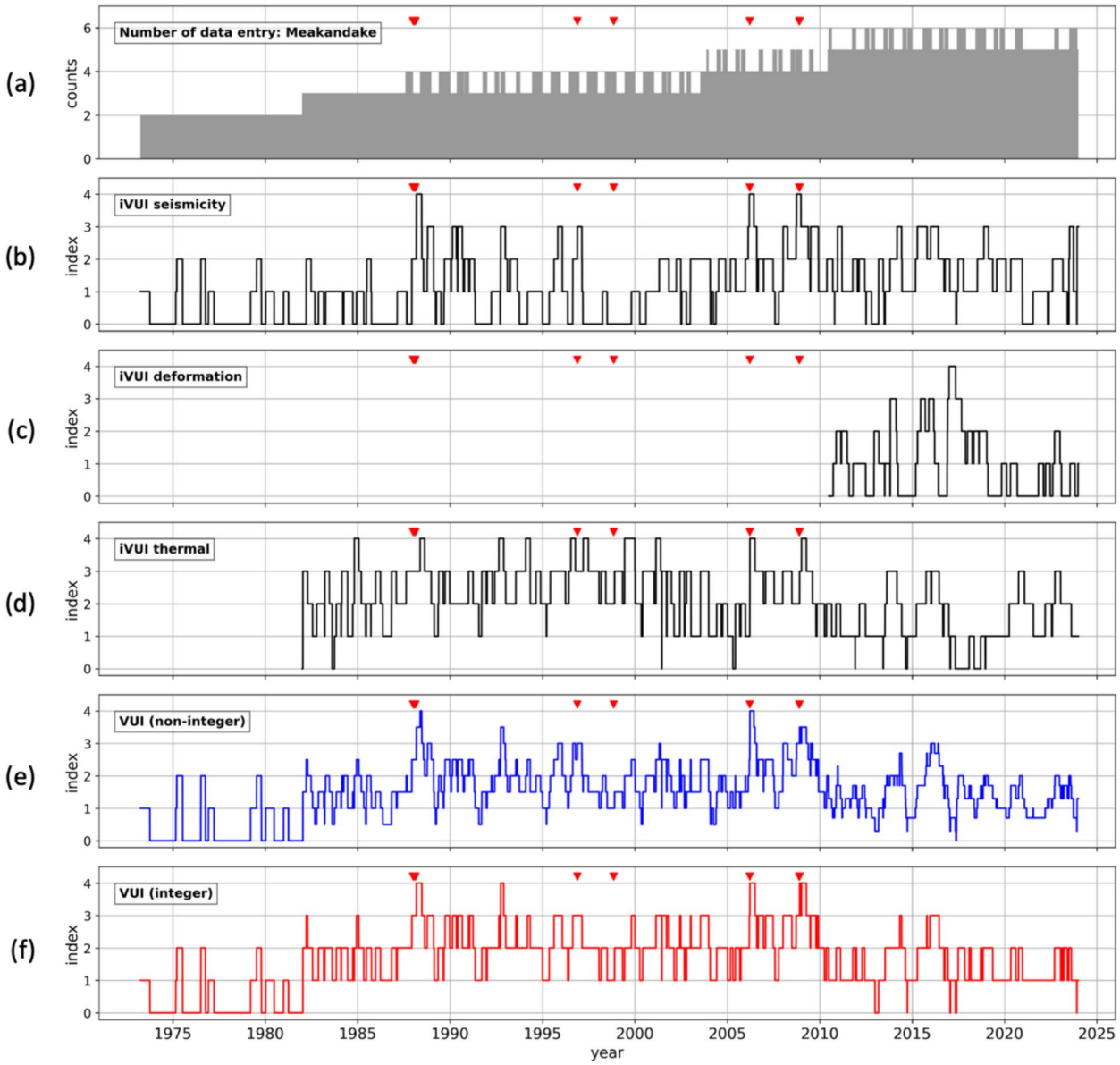


Fig. 6 Time series plots of analyzed results for Mt Meakandake. **a** Number of assessment Items; **b** Seismicity index; **c** Ground deformation index; **d** Thermal feature index; **e** Integrated VUI (non-integer); **f** Integrated VUI (rounded to integer). Inverted red triangles indicate the timing of eruptions

The 1992 instance of VUI 4 likely corresponds to an unrest event that did not culminate in eruption. In this case, the immediate trigger was the increase in seismic iVUI from 2 to 3 in October due to an earthquake swarm (Additional file 3: Fig. S7a-c), superimposed on already elevated plume heights at iVUI 4 (Additional file 3: Fig. S9e). By contrast, VUI values surrounding the 1996 and 1998 eruptions ranged from 1–3 and 1–2, respectively, without forming pronounced peaks. In particular, the subdued seismic and thermal activity around the 1998 eruption, as shown in Fig. 6 and Additional file 3: Fig. S7, is clearly reflected in the suppressed VUI. The 2006 and 2008 eruptions, conversely, were accompanied by pronounced seismic activity, producing distinct peaks reaching an integer VUI of 4. The relationship between these eruptions and the VUI is examined in detail in the Discussion section. Furthermore, between 2015 and 2017, increases in iVUI were observed across multiple monitoring parameters, including DLFE activity (Additional file 3: Fig. S7e), ground deformation (Additional file 3: Fig. S8), and magnetic field variations (Additional file 3: Fig. S11).

This period may be regarded as another isolated period of unrest, although the integer VUI remained at 3.

5 Discussion

5.1 Choice of thresholds

In the present study, iVUI evaluation thresholds for each record were, in principle, set such that the resulting proportion would be approximately 40% for iVUI 0, 30% for iVUI 1, 20% for iVUI 2, 9% for iVUI 3, and 1% for iVUI 4. While these values are not strongly justified by any physical rationale, the adopted proportions were selected to align with the qualitative definitions of the VUI levels proposed by Potter et al. (2015a), where VUI 0–4 correspond to "no unrest," "negligible unrest," "moderate unrest," "major unrest," and "heightened unrest," respectively. In this framework, higher levels are expected to represent progressively rarer and more significant unrest conditions.

This approach provides a practical means to maintain a balanced evaluation across different data Categories, although differences in temporal response characteristics among parameters are not explicitly accounted for. This approach, however, implicitly assumes that the dataset spanning over 50 years contains volcanic activity of varying intensities, with lower-intensity activity occurring more frequently. Such an assumption may not be appropriate when applying the method to shorter time series.

The 1% criterion for iVUI 4 is also arbitrary and can be adjusted according to operational objectives. As additional data accumulate, the underlying distribution may shift; therefore, the appropriateness of the thresholds should be reassessed and revised as needed. For the two volcanoes analyzed here, integer VUI 4 appeared twice at Tokachidake and four times at Meakandake, whereas the number of eruptive episodes (not the number of individual explosions) during the studied periods was three and five, respectively. These figures suggest that the chosen thresholds are reasonably consistent with the observed volcanic behavior.

It should be noted that the integration of multiple parameters using equal weighting represents a simplification, as different datasets may respond to volcanic unrest on different timescales and with varying sensitivities. For example, seismicity may exhibit rapid changes, whereas gas emissions or deformation may evolve more gradually. As such, the current framework does not explicitly account for these differences, and this should be considered when interpreting the results.

5.2 Opportunities for improving DLFE data usage

In this study, DLFE events at Meakandake were assessed based on the JMA's event list. However, Kurihara and Obara (2021) applied a Matched Filter analysis and detected 5484 events during the 14 years and 9 months from 2004 to 2018: approximately five times the number recorded in the JMA catalog (1146 events) during the corresponding period. This result indicates that utilizing the Matched Filter catalog could provide a more detailed representation of temporal variations in volcanic activity. In the present study, we primarily relied on raw JMA data without secondary processing, for simplicity. Nevertheless, future studies could enhance the representational ability of the VUI by incorporating such high-sensitivity detections.

For Tokachidake, the number of DLFE events recorded by JMA was limited, and therefore this parameter was not used in the current VUI assessment. Kurihara and Obara (2021) report that DLFE detection at Tokachidake is roughly one-tenth of that at Meakandake. Even so, the application of Matched Filter catalogs in the future is expected to allow the inclusion of DLFE as an evaluative parameter at Tokachidake as well.

5.3 Incorporation of magnetic field data

A notable aspect of this study is the inclusion of the total magnetic field data into the thermal Category. Direct crater temperature measurements are constrained by their limited temporal resolution, while plume height observations from a distance often suffer from missing records when the volcano is obscured by clouds. In contrast, continuous magnetic field monitoring helps to mitigate these limitations. Importantly, magnetic field changes capture subsurface thermal states rather than surface temperature, thus providing an independent proxy that complements surface-based observations. Nonetheless, because interpreting magnetic field variations inevitably requires some reliance on modeling, this dependence should be recognized and treated with due caution.

5.4 Challenges in the evaluation of Meakandake

During both the 2006 and 2008 eruptions of Meakandake, the integer VUI reached level 4. A closer look at the timeline, however, shows a different picture. In both cases, the index rose to level 3 before the eruption, but the transition to VUI 4 occurred only after the eruption had started (Fig. 7c). In 2006, seismicity was already elevated prior to the eruption. The immediate trigger for the integer VUI 4 was the sharp increase in plume height, which occurred three days after the eruption began (Additional file 3: Fig. S9). In 2008, seismic activity was also high before the eruption. In this case, the rise in the magnetic field record from iVUI 2 to 3 served as the trigger for the integer VUI 4 (Additional file 3: Fig. S11). Demagnetization had already been observed earlier, but the threshold was exceeded only after the second eruption on November 28, 2008.

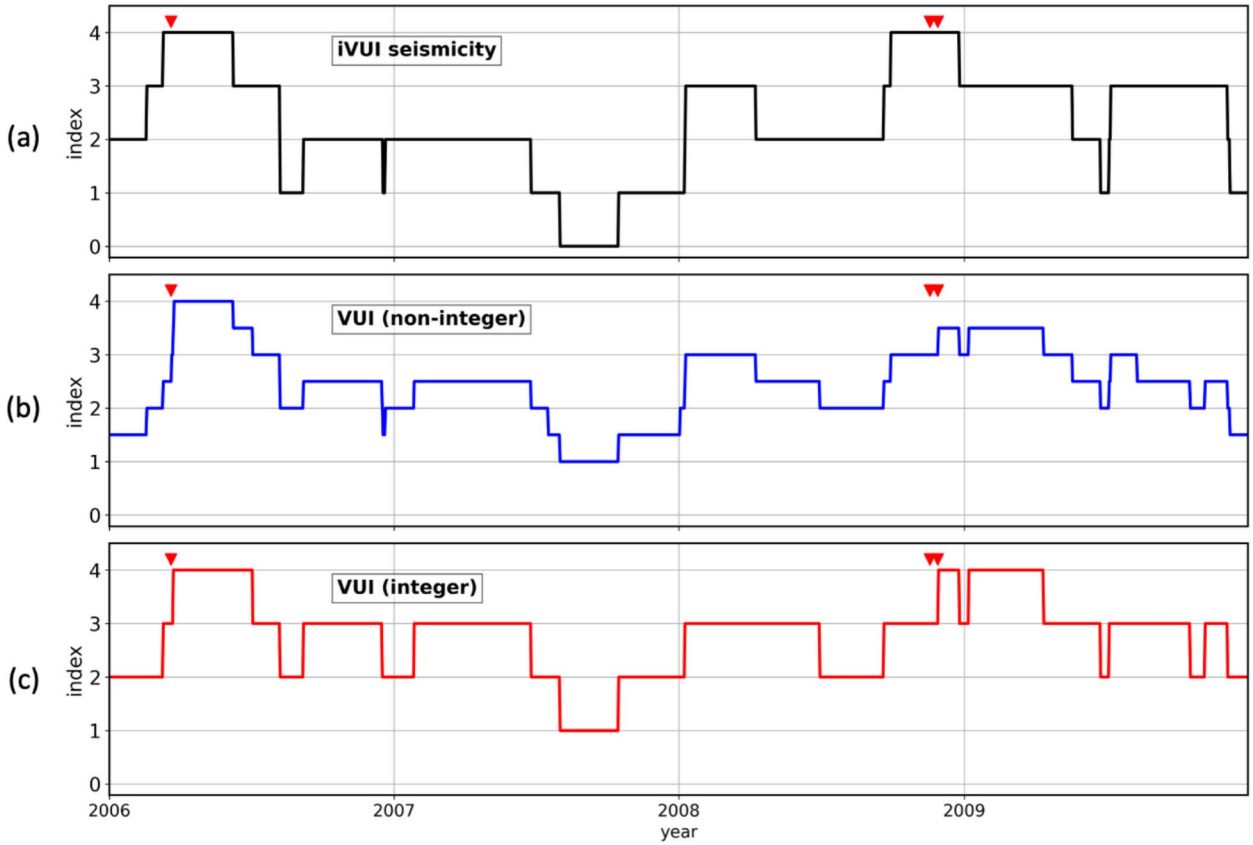


Fig. 7 Enlarged view of the time series from 2006 through 2009 for Mt Meakandake. Inverted red triangles indicate the timing of eruptions

Notably, in both cases, if the evaluation had been based solely on seismic activity, the integer VUI would have reached 4 prior to the eruption (Fig. 7a). This suggests that integrating multiple parameters smooths short-term variations and reduces pre-eruptive escalation, regardless of the length of the applied time window. However, it is important to recall that the VUI was not designed as a forecasting tool. Rather, its primary purpose is to characterize the level of volcanic activity. From this perspective, it is more appropriate to emphasize that activity levels corresponding to the eruption were captured as VUI 4 and sustained for a certain period of time.

The evaluation of Meakandake is still constrained by the limited set of data currently available, leaving substantial room for improvement. For instance, ground deformation records are confined to GNSS observations since 2010, making it difficult to assess the occurrence or scale of deformation during earlier eruptive episodes. In addition, this study could not incorporate datasets capable of detecting shallow crater-area deformation, which remains an important challenge for future work. A major limitation lies in the scarcity of continuous monitoring for the Nakamachineshiri crater, where only seismic activity and plume height are systematically recorded, thereby restricting the accuracy of assessments. Although not yet explored here, integrating approaches such as InSAR time-series analysis may offer a potential path forward.

In the 2008 Ponmachineshiri eruption, a few minutes of volcanic tremor were observed two days prior to the event, accompanied by tilt changes suggestive of crack opening directly beneath the crater (Aoyama and Ohshima 2015). While such signals have not yet been incorporated as evaluation parameters at this stage, their inclusion could enhance the short-term evaluation capability prior to eruptions.

5.5 Toward predictive applications of VUI

As emphasized by its developers, the VUI was not originally designed as a forecasting tool for volcanic eruptions (Potter et al. 2015a). However, they also pointed to the potential for predictive use, noting that "comparisons with the frequency of eruptions to unrest episodes can be undertaken, which, in turn, allows the testing and application of probabilistic models." To incorporate predictive elements into the VUI, the first requirement is

the accumulation of long-term, consistent, quantitative datasets that cover multiple eruptive episodes. Such datasets provide the foundation for improving the statistical robustness of evaluations. Ideally, they should allow for a robust assessment of the correspondence between datasets and eruptive events.

Volcanic activity is often observed as a progressive sequence from deeper to shallower processes. An evaluation framework that explicitly reflects this sequence would therefore be valuable. For example, in cases where DLFEs increase first and are followed by intensified shallow volcano-tectonic (VT) activity, using a longer evaluation window would allow the peaks of these signals to overlap, enabling the escalation of activity to be expressed as a continuous phenomenon. In addition, exploring multiple evaluation windows may improve the ability to capture temporally lagged, cascading processes that propagate across different timescales and influence longer-term activity patterns, representing a potential direction for future refinement of the framework. Although this study adopted the maximum value within each Category as the iVUI and did not test this approach, applying an averaging method to datasets that capture transitions from deep to shallow processes may provide a more accurate representation of temporal developments in activity.

For example, indicators of deeper magmatic activity may include DLFEs, increases in mantle-derived isotope components, an elevated C/S ratio in volcanic gases, and regional crustal deformation showing an inflationary trend. At intermediate depths, increased rates of VT earthquakes and enhanced SO_2 fluxes can serve as diagnostic signals. In the shallowest regions, phenomena such as a rise in low-frequency earthquakes, sudden changes in fumarolic activity, the development of steaming ground, elevated crater temperature, thermal demagnetization, and frequent volcanic tremors may provide important clues. It must be emphasized, however, that actual unrest episodes do not necessarily follow this pattern, and designing an evaluative framework that relies too heavily on a specific scenario entails the risk of undermining objectivity.

6 Conclusions

In this study, we provisionally introduced and applied the VUI (Potter et al. 2015a), to Mt Tokachidake and Mt Meakandake, two active volcanoes in northern Japan. Beyond the original formulation of the VUI, this study developed an operational evaluation framework that enables its application to long-term, multi-parameter volcanic monitoring datasets. By integrating more than 50 years of heterogeneous observations, including seismicity, ground deformation, thermal activity, and geochemical parameters, we demonstrated the feasibility of constructing a systematic platform for daily VUI evaluation based on a sliding time-window approach. In addition, we incorporated DLFE and long-baseline GNSS data to better evaluate deeper processes, and magnetic field records as an indicator of shallow thermal activity.

At Tokachidake, variations in the VUI correspond well with past eruptions and episodes of unrest, demonstrating the capability of the framework for tracking volcanic behavior over time. At Meakandake, the same framework enabled consistent quantitative evaluation of sub-eruptive unrest activity that were mostly associated with small phreatic eruptions.

The primary contribution of this study lies in the development of a computational and hierarchical implementation of the VUI, rather than the resulting index itself. This framework allows (1) the integration of diverse monitoring parameters into a structured hierarchical system, (2) daily evaluation of volcanic activity through sliding time windows, and (3) consistent comparison of unrest episodes over multi-decadal timescales within a unified quantitative framework.

Several limitations remain in the current implementation. Averaging across multiple Categories may limit its responsiveness, especially during the phases of escalating activity that appear only in the limited observational parameters. Although the VUI integrates parameters with diverse temporal resolutions and response characteristics, this aggregation may smooth short-term variations. The increasing availability of high-frequency observations from satellite remote sensing and drone-based measurements offers a promising avenue for improving temporal resolution and responsiveness. Because the VUI is not specifically designed for eruption forecasting or hazard assessment, careful distinction from the existing alert-level system is required during its societal implementation. One possible approach is the use of non-integer values, rather than discrete integer categories.

Future directions include optimizing the evaluation criteria for each individual volcanoes, and implementing automated real-time calculation systems to facilitate timely volcanic activity assessments and effective risk communication. Comparative studies across different volcanic settings will be also necessary to assess the generality of the framework. In the extended perspective, further refinement of data integration strategies may allow the VUI to incorporate a statistical forecasting capability. Recent advances in probabilistic frameworks, such as Bayesian network approach (e.g., Behr et al. 2025), provide complementary directions for future development.

Overall, this study represents the first implementation of a sliding-window, long-term, multi-parameter VUI evaluation platform for active volcanoes in Japan. It demonstrates that the VUI can be extended from a conceptual index to an operational framework for systematic volcanic activity assessment, providing a foundation for future monitoring, research, and information dissemination.

Abbreviations

DLFE	Deep low-frequency earthquake
DSAR	Displacement seismic amplitude ratio
GNSS	Global navigation satellite system
GSI	Geospatial Information Authority of Japan
HRO	Hokkaido Research Organization
InSAR	Interferometric synthetic aperture radar
JMA	Japan meteorological agency
JST	Japan standard time
OMI	Ozone monitoring instrument
RSAM	Real-time seismic amplitude measurement
TROPOMI	Tropospheric monitoring instrument
VAL	Volcanic alert level
VEI	Volcanic Explosivity Index
VT	Volcano-tectonic (earthquakes)
VUI	Volcanic unrest index

Supplementary Information

The online version contains supplementary material available at https://doi.org/10.1186/s40623-026-02486-9.

Supplementary Materials 1. Tokachidake worksheet. This spreadsheet provides the full calculation workflow of the VUI used in this study for Tokachidake. The file is implemented in Microsoft Excel (Microsoft Corporation) and includes functions specific to this environment; therefore, full functionality may not be preserved in other spreadsheet software. The file consists of multiple sheets organized as follows. The "worksheet" sheet provides an overview of the entire VUI worksheet, including the evaluation Categories, Items, Targets, and their corresponding evaluation criteria. The threshold values listed in this sheet are linked to the editable cells (highlighted in yellow) in the individual sheets. The "summary" sheet presents time-series data of the individual unrest indices (iVUI) for all Items. The column "# of Items" indicates the number of valid Items (i.e., the intermediate level of the assessment hierarchy), followed by columns for the non-integer and integer VUIs. The column "eruption" is used solely to indicate eruption timing as red triangles in the figures and does not carry numerical meaning. Subsequent sheets correspond to individual parameters. In each sheet, daily observational data are listed in columns highlighted in light green (blank or #N/A for missing data). Adjacent columns are used to calculate iVUI values. At the top of each sheet, summary tables show distributions of iVUI levels. Cells highlighted in yellow are user-editable threshold values; modifying these thresholds automatically updates the corresponding counts and proportions. Additional descriptions of the dataset, along with time-series plots, are provided in the upper right of each sheet.

Supplementary Material 2. Meakandake worksheet. This spreadsheet provides the full calculation workflow of the VUI used in this study for Meakandake. The spreadsheet structure and contents are the same as those of Supplementary Material 1.

Supplementary Material 3. Supplementary figures S1–S11.

Acknowledgements

We would like to express our sincere gratitude to the handling editor, Yuta Maeda, and to the reviewers, Joan Martí and Geoff Kilgour, for their careful reading of the manuscript and for their constructive and insightful comments, which have significantly improved the quality and clarity of this paper. We are also grateful to the Sapporo District Meteorological Observatory for serving as the point of contact for data provision from the Japan Meteorological Agency. We used GMT software (Wessel et al. 2019) and Matplotlib (Hunter 2007) to draw some of the figures. Some of the background maps in the figures are based on the shaded relief map from the GSI Maps (Geospatial Information Authority of Japan) provided on https://maps.gsi.go.jp.

Author contributions

TH and TO led the five-year research program that served as the foundation for this study. All authors contributed to discussions on the conceptual framework for introducing the VUI to Japanese volcanoes, which represents the central theme of this paper. TH, HA, R. Tanaka, TO, TM, R. Takahashi, and A. Takagi particularly contributed to developing the VUI criteria for Tokachidake and/or Meakandake. TH prepared the initial draft of the manuscript, and WK, A. Takagi, R. Tanaka, TM, R. Takahashi, and MY made substantial improvements. All authors approved the final version of the manuscript for submission.

Funding

This study was supported by the Ministry of Education, Culture, Sports, Science and Technology (MEXT) of Japan, under its The Second Earthquake and Volcano Hazards Observation and Research Program (Earthquake and Volcano Hazard Reduction Research).

Data availability

The datasets used for the VUI evaluation, together with their processed results and the evaluation criteria for each parameter, are provided in the Excel spreadsheets of Additional files 1 and 2.

Declarations

Competing interests

The authors declare that they have no competing interest.

Author details

[1]Institute of Seismology and Volcanology, Faculty of Science, Hokkaido University, Sapporo, Hokkaido 060-0810, Japan. [2]Aso Volcanological Laboratory, Institute for Geothermal Sciences, Graduate School of Science, Kyoto University, Kumamoto, Japan. [3]Graduate School of Science, The University of Tokyo, Bunkyo-ku, Tokyo, Japan. [4]Research Institute of Energy, Environment and Geology, Hokkaido Research Organization, Sapporo, Hokkaido, Japan. [5]Seismology and Volcanology Department, Japan Meteorological Agency, Minato-ku, Tokyo, Japan. [6]Research Center for Prediction of Earthquakes and Volcanic Eruptions, Graduate School of Science, Tohoku University, Sendai, Miyagi, Japan. [7]Multidisciplinary Resilience Research Center, Institute of Integrated Research, Institute of Science Tokyo, Meguro-ku, Tokyo, Japan. [8]Institute for Geothermal Sciences, Graduate School of Science, Kyoto University, Oita, Japan.

Received: 20 October 2025 Accepted: 11 June 2026
Published online: 30 June 2026

References

Aoyama H, Ohshima H (2015) Precursory tilt changes of small phreatic eruptions of Meakan-dake volcano, Hokkaido, Japan, in November 2008. Earth, Planets and Space 67:119. https://doi.org/10.1186/s40623-015-0289-9

Behr Y, Christophersen A, Miller C (2025) Probabilistic, multi-sensor eruption forecasting. Geophys Res Lett 52(8):e2024GL112029. https://doi.org/10.1029/2024GL112029

Carn SA, Fioletov VE, McLinden CA, Li C, Krotkov NA (2017) A decade of global volcanic SO2 emissions measured from space. Sci Rep 7:44095. https://doi.org/10.1038/srep44095

Caudron C, Girona T, Taisne B, Suparjan GH, Kristianto K (2019) Change in seismic attenuation as a long-term precursor of gas-driven eruptions. Geology 47(7):632–636. https://doi.org/10.1130/G46107.1

Endo ET, Murray T (1991) Real-time seismic amplitude measurement (RSAM): a volcano monitoring and prediction tool. Bull Volcanol 53:533–545. https://doi.org/10.1007/BF00298154

Geospatial Information Authority of Japan (2018) Crustal Deformations around Meakan Volcano. Report of the Coordinating Committee for Prediction of Volcanic Eruptions, 128, pp 5–19. https://www.jma.go.jp/jma/kishou/shingikai/ccpve/Report/128/kaiho_128_03.pdf **(in Japanese)**

Hasegawa T, Yamamoto A, Kamiyama H, Nakagawa M (2009) Gravity structure of Akan composite caldera, eastern Hokkaido, Japan: application of lake water corrections. Earth, Planets and Space 61:933–938. https://doi.org/10.1186/BF03353205

Hashimoto T, Nishimura M, Arita M, Yamamoto T, Ogiso M, Shigeno N, Okazaki N, Mogi T (2010) Heat accumulation beneath Tokachidake volcano as inferred from magnetic changes. Geophys Bull Hokkaido Univ 73: 269–280. (in Japanese) https://doi.org/10.14943/gbhu.73.269

Hunter JD (2007) Matplotlib: a 2D graphics environment. Comput Sci Eng 9(3):90–95. https://doi.org/10.1109/MCSE.2007.55

Japan Meteorological Agency (ed) (2013) National catalogue of the active volcanoes in Japan (the fourth edition). https://www.data.jma.go.jp/vois/data/filing/souran_eng/menu.htm

Japan Meteorological Agency (2026) Volcanic Warnings and Volcanic Alert Levels. https://www.jma.go.jp/jma/kishou/know/kazan/English/level.html. Accessed 25 Mar 2026

Johnston DM, Bebbington MS, Lai C-D, Houghton BF, Paton D (1999) Volcanic hazard perceptions: comparative shifts in knowledge and risk. Disaster Prev Manag 8(2):118–126. https://doi.org/10.1108/09653569910266166

Kurihara R, Obara K (2021) Spatiotemporal characteristics of relocated deep low-frequency earthquakes beneath 52 volcanic regions in Japan over an analysis period of 14 years and 9 months. J Geophys Res Solid Earth 126(10):e2021JB022173. https://doi.org/10.1029/2021JB022173

Minakami T (1960) Fundamental research for predicting volcanic eruptions (part 1) Earthquakes and crustal deformations originating from volcanic activities. Bull Earthq Res Ins 38:497–544

Moran SC, Newhall CG, Roman DC (2011) Failed magmatic eruptions: late-stage cessation of magma ascent. Bull Volcanol 73(2):115–122. https://doi.org/10.1007/s00445-010-0444-x

Mori T, Kazahaya K, Oppenheimer C, McGonigle AJS, Tsanev V, Olmos R, Ohwada M, Shuto T (2006) Sulfur dioxide fluxes from the volcanoes of Hokkaido, Japan. J Volcanol Geotherm Res 158:235–243. https://doi.org/10.1016/j.jvolgeores.2006.04.024

Newhall CG, Self S (1982) The volcanic explosivity index (VEI): an estimate of explosive magnitude for historical volcanism. J Geophys Res 87:1231–1238. https://doi.org/10.1029/JC087iC02p01231

Ozawa T (1965) Volcanic gases. Bull Volcanol Soc J 10:221–232. https://doi.org/10.18940/kazanc.10.10Special_221 **(in Japanese)**

Peers JB, Gregg CE, Lindell MK, Pelletier D, Romerio F, Joyner AT (2021) The economic effects of volcanic alerts—a case study of high-threat U.S. Volcanoes. Risk Anal 41(10):1759–1781. https://doi.org/10.1111/risa.13702

Potter SH, Scott BJ, Jolly GE, Johnston DM, Neall VE (2015a) A catalogue of caldera unrest at Taupo Volcanic Centre, New Zealand, using the Volcanic Unrest Index (VUI). Bull Volcanol 77:78. https://doi.org/10.1007/s00445-015-0956-5

Potter SH, Scott BJ, Jolly GE, Neall V, Johnston DM (2015b) Introducing the Volcanic Unrest Index (VUI): a tool to quantify and communicate the intensity of volcanic unrest. Bull Volcanol 77:77. https://doi.org/10.1007/s00445-015-0957-4

Sapporo Regional Headquarters, Volcanic Observation and Warning Center (2024) Volcanic activity of Meakandake in 2024. Bulletins on Volcanic Activity (Meakandake), pp 1-16. https://www.data.jma.go.jp/vois/data/report/monthly_v-act_doc/sapporo/2024y/105_24y.pdf **(in Japanese)**

Shinohara H, Saito G, Seki K, Kazahaya K, Kazahaya R, Morita M, Mannen K (2025) Chemical and Isotopic composition of volcanic gases in Japan (1991-2024). Open-File Report of the Geological Survey of Japan, AIST 765:24. **(in Japanese)**

Symonds RB, Gerlach TM, Reed MH (2001) Magmatic gas scrubbing: implications for volcano monitoring. J Volcanol Geotherm Res 108:303–341. https://doi.org/10.1016/S0377-0273(00)00292-4

Takahashi H, Shibata T, Yamaguchi T, Ikeda R, Okazaki N, Akita F (2012) Volcanic strain change prior to an earthquake swarm observed by groundwater level sensors in Meakan-dake, Hokkaido, Japan. J Volcanol Geotherm Res 215–216:1–7. https://doi.org/10.1016/j.jvolgeores.2011.11.006

Takahashi R, Shibata T, Murayama Y, Ogino T, Okazaki N (2015) Temporal changes in thermal waters related to volcanic activity of Tokachidake Volcano, Japan: implications for forecasting future eruptions. Bull Volcanol 77:2. https://doi.org/10.1007/s00445-014-0887-6

Takahashi K, Takakura S, Matsushima N, Fujii I (2018) Relationship between volcanic activity and shallow hydrothermal system at Meakandake volcano, Japan, inferred from geomagnetic and audio-frequency magnetotelluric measurements. J Volcanol Geotherm Res 349:351–369. https://doi.org/10.1016/j.jvolgeores.2017.11.019

Takahashi R, Okazaki N, Tamura M, Ogino T, Murayama Y (2019) The interaction of volcanic gas and deep magmatic fluid with shallow aquifers at Tokachidake volcano, Japan. J Volcanol Geotherm Res 388:106678. https://doi.org/10.1016/j.jvolgeores.2019.106678

Wessel P, Luis JF, Uieda L, Scharroo R, Wobbe F, Smith WHF, Tian D (2019) The generic mapping tools version 6. Geochem Geophy Geosyst 20(11):5556–5564. https://doi.org/10.1029/2019GC008515

Yamaguchi K, Tanaka R, Morita M, Mori T, Kazahaya R (2023) Sulfur dioxide flux measurement at Mount Tokachi, Japan, with TROPOspheric Monitoring Instrument. Front Earth Sci 11:1145343. https://doi.org/10.3389/feart.2023.1145343

Publisher's Note

Springer Nature remains neutral with regard to jurisdictional claims in published maps and institutional affiliations.